HHS Public Access

Author manuscript

Clin Cancer Res. Author manuscript; available in PMC 2019 January 29.

Published in final edited form as:

Clin Cancer Res. 2017 January 15; 23(2): 370–378. doi:10.1158/1078-0432.CCR-16-0150.

Differential expression and significance of PD-L1, IDO-1 and B7-H4 in human lung cancer

Kurt A. Schalper[1,2,3,*], **Daniel Carvajal-Hausdorf**[1], **Joseph McLaughlin**[2], **Mehmet Altan**[2], **Vamsidhar Velcheti**[4], **Patricia Gaule**[1], **Miguel F. Sanmamed**[5], **Lieping Chen**[5], **Roy S. Herbst**[2], and **David L. Rimm**[1,2]

[1]Department of Pathology, Yale School of Medicine.

[2]Medical Oncology section, Yale School of Medicine.

[3]Translational Immuno-oncology laboratory, Yale Cancer Center.

[4]Solid tumor oncology, Cleveland Clinic.

[5]Immunobiology, Yale School of Medicine

Abstract

Purpose: To determine the expression level, associations and biological role of PD-L1, IDO-1 and B7-H4 in non-small cell lung cancer (NSCLC).

Experimental design: Using multiplexed quantitative immunofluorescence (QIF), we measured the levels of PD-L1, IDO-1, B7-H4 and different tumor infiltrating lymphoycte (TIL) subsets in 552 stages I-IV lung carcinomas from 2 independent populations. Associations between the marker levels, TILs and major clinico-pathological variables were determined. Validation of findings was performed using mRNA expression data from The Cancer Genome Atlas (TCGA) and in vitro stimulation of lung adenocarcinoma A549 cells with IFN-γ and IL-10.

Results: PD-L1 was detected in 16.9% and 21.8% of cases in each population. IDO-1 was expressed in 42.6% and 49.8%; and B7-H4 in 12.8% and 22.6% of cases, respectively. Elevated PD-L1 and IDO-1 were consistently associated with prominent B and T-cell infiltrates, but B7-H4 was not. Co-expression of the 3 protein markers was infrequent and comparable results were seen in the lung cancer TCGA dataset. Levels of PD-L1 and IDO-1 (but not B7-H4) were increased by IFN-γ stimulation in A549 cells. Treatment with IL-10 upregulated B7-H4, but did not affect PD-L1 and IDO-1 levels.

Conclusions: PD-L1, IDO-1 and B7-H4 are differentially expressed in human lung carcinomas and show limited co-expression. While PD-L1 and IDO-1 are associated with increased TILs and IFN-γ stimulation, B7-H4 is not. The preferential expression of discrete immune evasion pathways in lung cancer could participate in therapeutic resistance and support design of optimal clinical trials.

[*]To whom correspondence should be addressed: Kurt A. Schalper, M.D./Ph.D., Assistant Professor of Pathology and Medicine (Medical Oncology), Yale School of Medicine, Director Translational Immuno-oncology Laboratory, Yale Cancer Center, Office Address: 333 Cedar St. SHMI 234C, New Haven, CT 06520-8023, Office Phone: 203-785-4719, Lab Address: 310 Cedar St. BML113, New Haven, CT 06520-8023, Lab Phone: 203-737-3588.

Conflicts of interest: All authors have declared no conflict of interest with the data presented.

Introduction

Despite progress in the understanding of the molecular basis and development of targeted therapies, lung cancer is still the leading cause of cancer related morbidity and mortality worldwide (1–2). Targeted therapies using tyrosine kinase inhibitors (TKIs) are safe and effective, but they can be used in a relatively small proportion of patients with advanced disease harboring key actionable mutations such as EGFR, ALK and ROS1 (3). In addition, response to TKIs is inevitably followed by acquired resistance, typically only months after treatment onset.

Upregulation of immune inhibitory mechanisms such as co-regulatory ligands/receptors and tolerogenic enzymes by cancer cells allow tumors escape from immune attack. Novel anti-cancer immunotherapies blocking immune co-inhibitory pathways (also referred to as “immune checkpoints”) such as PD-1 and CTLA-4 have shown prominent and durable responses in diverse malignancies. In particular, blockade of the PD-1 receptor or its ligand PD-L1 induces objective responses in about 20% of patients with heavily pre-treated non-small cell lung cancer (NSCLC) with median duration >12 months and some cases with ongoing responses lasting over 2–3 years (4–7). The success of these therapies uncovered the power of blocking immune inhibitory pathways. Diverse studies have found that expression of PD-L1 by immunohistochemistry (IHC), pre-existence of tumor infiltrating lymphocytes (TILs) and increased nonsynonymous mutations or predicted neoantigens are associated with benefit to PD-1 axis blockers (8–11). These findings support the notion that adaptive tumor PD-L1 upregulation, secondary to anti-tumor immune pressure is associated with lymphocyte re-invigoration using these therapies. Because only a fraction of patients show objective benefit from PD-1 pathway blockade, development of therapeutic strategies to effectively treat primary resistant tumors lacking PD-L1 expression and immune infiltration are needed. Efforts are now focusing on combination strategies to block additional immune suppressive signals and activate co-stimulatory receptors to increase response rates, prolong responses, and counteract resistance to monotherapy regimens. The expression and biological role of additional potentially actionable immune inhibitory targets beyond PD-L1 in lung cancer are not well understood.

Indoleamine-2,3-dioxygenase 1 (IDO-1), is the rate-limiting enzyme in tryptophan catabolism and exerts a potent immune suppressive effect through local inhibition of T lymphocytes and other immune cells (12–13). T-cells exposed to tryptophan depletion activate GCN2 kinase, a sensor of low amino acid content that induces a stress response, resulting in impaired T-cell proliferation and effector functions. In addition, tryptophan catabolites such as kynurenine reduce survival of CD4 T helper cells and promote regulatory T cell differentiation (12–13). IDO-1 has been shown to induce immune suppressive effects and favor tumor progression in animal models of lung cancer (14). Variable levels of IDO-1 have been found in human solid tumors including melanomas, gliomas and carcinomas from different locations (15–16). Blockade of IDO-1 using small molecule inhibitors in combination with immune checkpoint blockade induces prominent anti-tumor responses in mouse models (17–19) and reversal of tumor-associated immunosuppression by 1-methyl-D-Tryptophan (1-MDT [Indoximod, NLG8189]) appears to be dependent on host IDO-1

expression (12). Diverse early phase trials investigating IDO inhibition with 1-MDT and other compounds alone or in combination are underway.

B7-H4 is one of the most recently identified members of the B7 homologue family of immune co-regulatory molecules that encompasses also PD-L1 (also known as B7-H1 or CD274) and PD-L2 (also known as B7-DC or CD273) (20–22). Although the receptor for B7-H4 remains unknown, in vitro studies indicate a potent immunosuppressive role and its expression has been found with variable levels in diverse human malignancies, including lung cancer (23–25). Blockade of B7-H4 using recombinant monoclonal antibodies enhances antigen-specific T-cell activation and reduces tumor growth in a humanized mice model of ovarian cancer (26) and therapeutic antibody conjugates targeting human B7-H4 are under development (27).

Despite their known expression in human lung cancer and clear therapeutic potential the association between PD-L1, IDO-1 and B7-H4 expression remains unclear. Here, we measured the levels of these immune targets and study their association with immune cell infiltration in two lung cancer populations using objective methods and validated antibodies. To explore their biological role we also studied the association between the markers, clinico-pathological characteristics and outcome. Finally, we confirmed the relationship between the targets in the TCGA lung cancer dataset and their modulation by cytokines in cultured lung cancer cells.

Materials and Methods

Patients, cohorts and tissue microarrays

Samples from 2 previously described retrospective collections of lung cancer, one from Yale University (cohort #1) and other from Greece (cohort #2), represented in tissue microarrays (TMAs) were used (28–29). The first cohort includes 202 samples and the second set includes 350 lung carcinomas. Detailed clinico-pathological characteristics of the cohorts were recently communicated (28–29) and are shown in the supplemental Table S1. TMAs were prepared using 0.6 mm tissue cores, each in 2-fold redundancy using standard procedures. The actual number of samples analyzed for each study is lower, due to unavoidable loss of tissue or the absence or limited tumor cells in some spots as is commonly seen in TMA studies. All tissue was used after approval from the Yale Human Investigation Committee protocol #9505008219, which approved the patient consent forms or in some cases waiver of consent.

Quantitative immunofluorescence (QIF)

We measured the levels of PD-L1 (E1L3N, Cell Signaling), IDO-1 (1F8.2, Millipore), B7-H4 (D1M8I, Cell Signaling), CD3 (clone E272, Novus Biologicals), CD8 (clone C8/144B, DAKO), CD20 (clone L26, DAKO) and pancytokeratin (AE1/AE3, DAKO) using QIF in TMA slides containing the cohort cases.

PD-L1, IDO-1 and B7-H4 were stained in serial sections from the TMA blocks, using a previously described protocol with simultaneous detection of cytokeratin and DAPI (29). Briefly, antigen retrieval was with citrate buffer pH 6.0 for 20 min at 97°C in a pressure-

boiling container and blocking was performed with 0.3% bovine serum albumin in 0.05% Tween solution for 30 minutes. Primary antibodies were incubated overnight at a titer of 1:1600 for PD-L1, 1:200 for B7-H4 and 1:250 for IDO-1. Secondary antibody for cytokeratin was Alexa 546-conjugated goat anti-mouse or anti-rabbit (Invitrogen Molecular Probes, Eugene, OR, USA). Cyanine 5 (Cy5) directly conjugated to tyramide (FP1117; Perkin-Elmer) at a 1:50 dilution was used for target antibody detection (29). In selected experiments, PD-L1 and IDO-1 or B7-H4 were simultaneously stained in NSCLC specimens.

CD3, CD8, CD20 and cytokeratin were simultaneously stained using a sequential staining protocol, as previously described (28). Briefly, freshly cut TMA sections were deparaffinized and subjected to antigen retrieval using pH=8.0 EDTA buffer (Sigma-Aldrich, St Louis, MO, USA) and boiled for 20 min at 97°C in a pressure-boiling container (PT module, Lab Vision, Thermo Scientific, Waltham, MA, USA). Slides were then incubated with dual endogenous peroxidase block (DAKO #S2003, Carpinteria, CA, USA) for 10 min at room temperature and subsequently with a blocking solution containing 0.3% bovine serum albumin in 0.05% Tween solution for 30 minutes. Residual horseradish peroxidase activity between incubations with secondary antibodies was eliminated by exposing the slides twice for 7 min to a solution containing benzoic hydrazide (100 mM) and hydrogen peroxide (50 mM) in 10 ml of PBS. Isotype specific, fluorophore-conjugated antibodies were used for signal detection and nuclei were highlighted using DAPI (28).

Fluorescence signal quantification and cases stratification

Quantitative measurement of the fluorescent signal was performed using the AQUA® method of QIF, as previously described (28–30). Briefly, the QIF score of each fluorescence channel was calculated by dividing the target marker pixel intensities by the area of the desired compartment. Scores were normalized to the exposure time and bit depth at which the images were captured, allowing scores collected at different exposure times to be comparable. A pathologist (KAS) visually examined the stained slides and cases with artifacts were excluded. The immune target scores considered the signal detected in the tumor (cytokeratin positive) or stromal (cytokeratin negative) compartment and cases with less than 5% tumor were excluded from the analysis. Measurement of TIL markers considered the levels detected in the whole tumor sample (e.g. tumor and stroma). For stratification purposes, cases were considered as target expressers when the QIF score was above the signal detection threshold determined using the negative control preparations and visual inspection (28–30). The levels of CD3, CD8 and CD20 were classified as high/low using the median score as cutpoint.

Cell culture and cytokine treatment

Human A549 lung carcinoma cells were plated in 100mm^2 petri dish and allowed to reach 70–80% confluence, as previously reported (30). Cells were washed 3x with PBS and incubated for 24 h in serum free RPMI 1640. Cells were treated with either/and recombinant Interferon-γ (IFN-γ [15ng/ml]) or Interleukin-10 (IL-10 [50ng/ml]) for 24 h in serum free RPMI 1640 and harvested for protein isolation. Controls included both normal serum concentration and serum-starved cells.

Protein measurement by Western blot

Protein extraction and immunoblotting of cultured cells was performed as previously reported (30). Briefly, harvested cells were lysed in RIPA buffer supplemented with 1x protease inhibitors and 1 mM sodium orthovanadate. Centrifugation was performed at 12,000 rpm for 10 minutes at 4°C to remove cellular debris. Protein quantification was performed using the Bicinchoninic acid (BCA) assay (Pierce). Isolated protein in sample buffer was heated to 95°C for 5 minutes and proteins were resolved on 4–12% Bis-Tris Gels (Invitrogen) at 45mA maximum V for 1.5hrs. Protein was transferred to nitrocellulose membrane using 1x Nupage Transfer Buffer at 50V, maximum mA for 2hrs. The membrane was blocked with 5% milk in 0.05% TBST at RT for 1 hour, then incubated overnight at 4°C in blocking solution with 1:500 antibody dilution of anti-PD-L1, 1:1000 anti-B7-H4 and 1:1000 anti IDO-1. Membranes were washed 3x in 0.05% TBST and incubated with anti-rabbit/mouse as appropriate for 1hr at RT. Detection of resolved protein was performed using Super Signal® West Pico Chemiluminescent Substrate (Thermo Scientific).

Statistical analyses

QIF signal differences between groups were analyzed using t-test for continuous variables and chi-square test for categorical variables. Linear regression coefficients were calculated to determine the association between continuous scores. Survival analysis based on the markers expression was performed using Kaplan-Meier analyses with log rank test and overall survival as endpoint. Statistical significance was considered at $P<0.05$ and analyses were performed using JMP® Pro software (version 9.0.0, 2010, SAS Institute Inc.) and GraphPad Prism v6.0 for Windows (GraphPad Software, Inc). All statistical tests were two-sided.

Results

Assay validation and performance

Validation of the PD-L1 protein assay was reported in a previous publication from our group (30). Stringent validation of the IDO-1 and B7-H4 assays using parental cells, cell line transfectants and endogenous tissue controls is shown in the supplementary Figure S1.

Expression of PD-L1, IDO-1, B7-H4 and TILs in lung cancer

In lung cancer PD-L1, IDO-1 and B7-H4 showed distinct staining patterns. As shown in Figure 1A, PD-L1 and B7-H4 showed a predominant cytoplasmic/membranous distribution. As expected for a cytosolic enzyme, IDO-1 expression showed a predominant perinuclear staining pattern (Figure 1A, center). The levels of all three markers were significantly higher in the tumor compartment than in stromal cells (Figure 1B). For PD-L1 and IDO-1 the stromal signal was typically focal and positively associated with the tumor signal (Linear correlation coefficient [R^2] of 0.64 in the first cohort and 0.66 in the second cohort for PD-L1 and R^2= 0.65 and 0.82 for IDO-1, respectively). B7-H4 staining was detected almost exclusively in tumor cells (R^2=0.25 and 0.39 in each cohort, respectively). Using a previously validated multiplex QIF staining panel including the markers DAPI, cytokeratin, CD3, CD8 and CD20 (28), we identified tumors with variable lymphocyte infiltration

patterns. As shown in Figure 1C, some cases displayed low/minimal TILs (Figure 1C, left panel), other prominent CD3+ T-cells (middle panel) or mixed inflammation with abundant CD20+ B-cell infiltration (right panel).

The levels of the markers in the lung cohorts showed a continuous distribution. Using a cutpoint established from scores obtained in negative control preparations and the visual detection threshold, PD-L1 signal was identified in 16.9% of cases in the first cohort (Figure 2A) and 21.8% of cases in the second collection (Figure 2B). IDO-1 was expressed in 42.6% of cases in cohort #1 (Figure 2C) and 49.8% in the validation set (Figure 2D) and B7-H4 was found in 12.8% and 22.6%, respectively (Figures 2E and F).

Association between PD-L1, IDO-1, B7-H4 and TILs in lung cancer

As previously reported by our group using a different PD-L1 assay targeting the extracellular protein domain (antibody clone 5H1, [29]), tumor PD-L1 expression was positively associated with lymphocyte infiltration. In particular, PD-L1 signal was independently associated with elevated CD3, CD8 or CD20 positive lymphocytes in both cohorts (Tables 1 and 2). No consistent association was seen between PD-L1 expression and sex, age, clinical stage and histology. IDO-1 was also positively associated with all three TIL markers in both cohorts, but not with other clinico-pathological variables (Tables 1 and 2). Tumor expression of B7-H4 was consistently associated with squamous cell histology, but not with the presence of lymphocyte infiltration or other variables. Despite their association with TILs, expression of the markers was not consistently associated with 5-year overall survival, suggesting a limited prognostic effect (supplementary Figure S2).

PD-L1, IDO-1 and B7-H4 are infrequently co-expressed in lung cancer

Samples from lung carcinomas with prominent levels of one of the markers had typically low levels of the other. Representative examples of 3 tumors with mutually exclusive expression of PD-L1, IDO-1 and B7-H4 are shown in Figure 3A-C. Consistent with the visual assessment and using the continuous QIF scores for each marker, we identified only few cases with concomitant expression of PD-L1 and IDO-1 (Figure 3D-E). Overall, the proportion of cases co-expressing PD-L1 and IDO-1 was 7.1% in the first cohort and 10.9% in the second group. Cases showing co-expression of PD-L1 and B7-H4 were only 3.2 and 3.4% in each cohort, respectively; and cases with detectable levels of IDO-1 and B7-H4 were 6.1 and 9.8% of tumors. Comparable results were seen by simultaneous co-staining of PD-L1 and IDO-1 or B7-H4 in lung carcinomas (supplementary Figure S3).

To rule out possible bias induced by limited tumor representation using TMAs and/or the effect of marker heterogeneity, we analyzed the levels of PD-L1, IDO-1 and B7-H4 mRNA from the TCGA lung cancer dataset obtained by RNA-sequencing from whole tissue section tumor samples (31). As shown in the Figure 4, a similarly restricted co-expression between the markers was observed in both squamous carcinomas (Figure 4A, N=178) and primary lung adenocarcinomas (Figure 4B, N=230).

Modulation of PD-L1, IDO-1 and B7-H4 by cytokines in lung cancer cells.

In efforts to explain the nearly mutually exclusive pattern of expression at both the protein and mRNA levels, we examined factors inducing their expression. Previous studies have indicated that PD-L1 and IDO-1 expression is induced by IFN-γ stimulation (9, 10, 16) and B7-H4 upregulation occurs after IL-6 or IL-10 stimulation in cultured monocytic cells (24). To confirm the modulation of the targets in human tumor cells, we treated A549 lung adenocarcinoma cells for 24 h with 15 ng/ml recombinant IFN-γ, 50 ng/ml IL-10 or the combination. As shown in supplementary Figure S4, control serum-starved A549 cells lack detectable levels of PD-L1, IDO-1 and B7-H4 protein by Western blot. Treatment with IFN-γ prominently increases the levels of PD-L1 and IDO-1, but not of B7-H4. Reciprocally, treatment with IL-10 increases B7-H4, but does not alter the levels of PD-L1 and IDO-1. Treatment with the combination of IFN-γ and IL-10 mimics the effect of IFN-γ alone. Cell lines used in this study were purchased in the American Type Culture Collection (ATCC) and authentication was performed every 3–6 months using the GenePrint® 10 System in the Yale University DNA Analysis Facility.

Discussion

Using multiplexed QIF, we show that PD-L1, IDO-1 and B7-H4 are differentially expressed and infrequently co-expressed in human lung cancer. The markers are located preferentially in tumor cells and show distinct association with lymphocyte infiltration. While PD-L1 and B7-H4 were found in 10–25% of cases, IDO-1 expression was detected in over 40% of tumors in 2 independent populations. The proportion of cases showing PD-L1 expression reported here is lower than in our previous study using the same retrospective lung cancer collections (29). This difference may be explained by the use of a different PD-L1 monoclonal antibody in this study recognizing the intracellular protein domain (clone E1L3N) and not an extracellular epitope as in our previous report (clone 5H1) or other differences between the two antibodies. In support of this notion, recent work by our group using whole tissue section specimens confirmed the frequent discordance between validated PD-L1 assays in lung carcinomas (32).

The proportion of lung cancer cases showing IDO-1 and B7-H4 expression is relatively lower than in previous reports. In NSCLC, IDO-1 protein has been detected in 67–79% of cases using chromogenic IHC (15–16) and B7-H4 was found in 43% of lung cancers (25). The determinants for this apparent discrepancy are uncertain and could be related with the use of relatively small tissue fragments in our study. However, the rigorous validation of our assays and the objective/quantitative platform used support a precise measurement of the targets. The relative high frequency of IDO-1 expression found in lung cancers supports the possibility of using available (small molecule) IDO inhibitors as anti-cancer immunostimulatory therapy.

Notably, the markers showed an exclusive pattern with infrequent co-expression, suggesting that most lung tumors use preferentially only one immune evasion mechanism/pathway. Our results also suggest the possibility of alterations of these targets as possible mechanisms of acquired resistance to PD-1 axis therapies.

Consistent with their previously reported induction by Th1/IFN-γ signaling (9, 10, 16), elevated PD-L1 and IDO-1 were significantly associated with high CD3 and CD8-positive T-lymphocyte infiltration. Increased PD-L1 and IDO-1 were also associated with high CD20-positive B lymphocytes. Our in vitro results also confirm the adaptive induction of PD-L1 and IDO-1 by IFN-γ in cultured adenocarcinoma cells. Therefore, the frequent lack of co-expression of PD-L1 and IDO-1 seen in lung tumors both at the protein and mRNA level in 3 different populations (e.g. 2 retrospective cohorts and the TCGA set) could be mediated by additional signaling events occurring in the tumor or tumor microenvironment. For instance, expression of PD-L1 can be modulated by IFN-α, IFN-β, GM-CSF, VEGF, LPS, IL-4 and IL-10 (10). IDO-1 levels are sensitive to COX-2 signaling through prostaglandin E2, TGF-β and nitric oxide (33). Future studies will be required to clarify this apparent contradiction. On the contrary and as expected by its previously identified induction by Th2/IL-10 signaling (24), B7-H4 was not associated with PD-L1, IDO-1 or increased TILs. The expression of B7-H4 in non- or less inflamed tumors suggests the possibility of using this molecule as therapeutic target in these malignancies (10, 29). In addition, and as previously described (20), B7-H4 levels were higher in squamous cell carcinomas than in the other histological variants of lung cancer, suggesting a therapeutic opportunity for this aggressive malignancy with limited available therapies. Although previously shown to have marked immune-suppressive effect in cultured cells and animal models of ovarian cancer (23–26), the precise biological role of B7-H4 in lung cancer requires further investigation.

Despite their association with TILs, expression of PD-L1, IDO-1 and B7-H4 was not consistently associated with survival. The absence of prognostic value of the markers may not be a limitation for their possible role as predictive biomarkers. For instance, EGFR mutations and ALK rearrangements are highly predictive of response to targeted therapies in lung adenocarcinomas, but their prognostic value is limited.

Our study has a number of limitations. First, we included retrospectively collected samples from cases with variable follow-up, different treatments and lacking molecular/genomic annotation. However, we found comparable results in both collections, suggesting that our findings are independent from treatment and molecular subtype. Also, our cases were represented in TMA format, which may induce under or overrepresentation of the marker levels due to tumor heterogeneity. However, the comparable results seen in the TCGA dataset using mRNA measurements in whole tissue section tumor samples supports the validity of our findings.

Although a myriad of additional immune suppressive ligands and receptors have been described and could play a relevant role in lung cancer, our results suggest the opportunity for optimization of immunotherapy through measurement of the drug targets in pre-treatment tumor samples.

Supplementary Material

Refer to Web version on PubMed Central for supplementary material.

Acknowledgments:

We would like to thank Nikita Mani for experimental support and Lori Charette from the Yale Pathology Tissue Services for production of optimal TMAs and tissue slides.

Funding information: This research was supported by a Stand Up To Cancer - American Cancer Society Lung Cancer Dream Team Translational Research Grant (Grant Number: SU2C-AACR-DT17–15). Stand Up to Cancer is a program of the Entertainment Industry Foundation. Research grants are administered by the American Association for Cancer Research, the scientific partner of SU2C. This work was also funded by the Yale SPORE in Lung Cancer (P50CA196530) Career Development Program award (to KAS), a Lung Cancer Research Foundation grant (to KAS) and the Yale Cancer Center Support Grant (P30CA016359).

References and Notes:

1. Brambilla E, TW, Lung cancer In: World Cancer Report, Stewart BW, Wild CP (Eds), 2014; World Health Organization, Lyon.
2. Siegel RL, Miller KD and Jemal A Cancer statistics. CA Cancer J Clin, 2015; 65:5–29. [PubMed: 25559415]
3. Rothschild SI. Targeted Therapies in Non-Small Cell Lung Cancer-Beyond EGFR and ALK. Cancers (Basel) 2015;7:930–49. [PubMed: 26018876]
4. Herbst RS, Soria JC, Kowanetz M, Fine GD, Hamid O, Gordon MS, et al. Predictive correlates of response to the anti-PD-L1 antibody MPDL3280A in cancer patients. Nature 2014; 515:563–7. [PubMed: 25428504]
5. Garon EB, Rizvi NA, Hui R, Leighl N, Balmanoukian AS, Eder JP, et al. Pembrolizumab for the treatment of non-small-cell lung cancer. N Engl J Med. 2015;372:2018–28. [PubMed: 25891174]
6. Rizvi NA, Mazières J, Planchard D, Stinchcombe TE, Dy GK, Antonia SJ, et al. Activity and safety of nivolumab, an anti-PD-1 immune checkpoint inhibitor, for patients with advanced, refractory squamous non-small-cell lung cancer (CheckMate 063): a phase 2, single-arm trial. Lancet Oncol. 2015;16:257–65. [PubMed: 25704439]
7. Brahmer J, Reckamp KL, Baas P, Crinò L, Eberhardt WE, Poddubskaya E, et al. Nivolumab versus Docetaxel in Advanced Squamous-Cell Non-Small-Cell Lung Cancer. N Engl J Med. 2015;373:123–35. [PubMed: 26028407]
8. Topalian SL, Hodi FS, Brahmer JR, Gettinger SN, Smith DC, McDermott DF, et al. Safety, activity, and immune correlates of anti-PD-1 antibody in cancer. N Engl J Med. 2012;366:2443–54. [PubMed: 22658127]
9. Tumeh PC, Harview CL, Yearley JH, Shintaku IP, Taylor EJ, Robert L, et al. PD-1 blockade induces responses by inhibiting adaptive immune resistance. Nature 2014;515:568–71. [PubMed: 25428505]
10. Sznol M and Chen L. Antagonist antibodies to PD-1 and B7-H1 (PD-L1) in the treatment of advanced human cancer. Clin Cancer Res. 2013;19:1021–34. [PubMed: 23460533]
11. Rizvi NA, Hellmann MD, Snyder A, Kvistborg P, Makarov V, Havel JJ, et al. Cancer immunology. Mutational landscape determines sensitivity to PD-1 blockade in non-small cell lung cancer. Science 2015;348:124–8. [PubMed: 25765070]
12. Platten M, von Knebel Doeberitz N, Oezen I, Wick W, Ochs K. Cancer Immunotherapy by Targeting IDO1/TDO and Their Downstream Effectors. Front Immunol. 2015;5:673. [PubMed: 25628622]
13. Munn DH, Mellor AL. Indoleamine 2,3 dioxygenase and metabolic control of immune responses. Trends Immunol. 2013;34:137–43. [PubMed: 23103127]
14. Smith C, Chang MY, Parker KH, Beury DW, DuHadaway JB, Flick HE, et al. IDO is a nodal pathogenic driver of lung cancer and metastasis development. Cancer Discov. 2012;2:722–35. [PubMed: 22822050]
15. Théate I, van Baren N, Pilotte L, Moulin P, Larrieu P, Renauld JC, et al. Extensive profiling of the expression of the indoleamine 2,3-dioxygenase 1 protein in normal and tumoral human tissues. Cancer Immunol Res. 2015;3:161–72. [PubMed: 25271151]

16. Xie Q, Wang L, Zhu B, Wang Y, Gu J, Chen Z. The expression and significance of indoleamine −2,3 -dioxygenase in non-small cell lung cancer cell. Zhongguo Fei Ai Za Zhi. 2008;11:115–9. [PubMed: 20727279]
17. Wainwright DA, Chang AL, Dey M, Balyasnikova IV, Kim CK, Tobias A, et al. Durable therapeutic efficacy utilizing combinatorial blockade against IDO, CTLA-4, and PD-L1 in mice with brain tumors. Clin Cancer Res. 2014;20:5290–301. [PubMed: 24691018]
18. Spranger S, Koblish HK, Horton B, Scherle PA, Newton R, Gajewski TF. Mechanism of tumor rejection with doublets of CTLA-4, PD-1/PD-L1, or IDO blockade involves restored IL-2 production and proliferation of CD8(+) T cells directly within the tumor microenvironment. J Immunother Cancer. 2014; 2:3. [PubMed: 24829760]
19. Li M, Bolduc AR, Hoda MN, Gamble DN, Dolisca SB, Bolduc AK, et al. The indoleamine 2,3-dioxygenase pathway controls complement-dependent enhancement of chemo-radiation therapy against murine glioblastoma. J Immunother Cancer. 2014;2:21. [PubMed: 25054064]
20. Sica GL, Choi IH, Zhu G, Tamada K, Wang SD, Tamura H, et al. B7-H4, a molecule of the B7 family, negatively regulates T cell immunity. Immunity 2003;18:849–61. [PubMed: 12818165]
21. Prasad DV, Richards S, Mai XM, Dong C. B7S, a novel B7 family member that negatively regulates T cell activation. Immunity 2003;18:863–73. [PubMed: 12818166]
22. Zang X, Loke P, Kim J, Murphy K, Waitz R, Allison JP. B7x: a widely expressed B7 family member that inhibits T cell activation. Proc Natl Acad Sci U S A. 2003;100:10388–92. [PubMed: 12920180]
23. Yi KH and Chen L. Fine tuning the immune response through B7-H3 and B7-H4. Immunol Rev. 2009; 229:145–51. [PubMed: 19426220]
24. He C, Qiao H, Jiang H, Sun X. The inhibitory role of b7-h4 in antitumor immunity: association with cancer progression and survival. Clin Dev Immunol. 2011;2011:695834. [PubMed: 22013483]
25. Sun Y, Wang Y, Zhao J, Gu M, Giscombe R, Lefvert AK, et al. B7-H3 and B7-H4 expression in non-small-cell lung cancer. Lung Cancer. 2006;53:143–51. [PubMed: 16782226]
26. Dangaj D, Lanitis E, Zhao A, Joshi S, Cheng Y, Sandaltzopoulos R, et al. Novel recombinant human b7-h4 antibodies overcome tumoral immune escape to potentiate T-cell antitumor responses. Cancer Res. 2013;73:4820–9. [PubMed: 23722540]
27. Leong SR, Liang WC, Wu Y, Crocker L, Cheng E, Sampath D, et al. An anti-B7-H4 antibody-drug conjugate for the treatment of breast cancer. Mol Pharm. 2015; 12:1717–29. [PubMed: 25853436]
28. Schalper KA, Brown J, Carvajal-Hausdorf D, McLaughlin J, Velcheti V, Syrigos KN, et al. Objective measurement and clinical significance of TILs in non-small cell lung cancer. J Natl Cancer Inst. 2015;107.
29. Velcheti V, Schalper KA, Carvajal DE, Anagnostou VK, Syrigos KN, Sznol M, et al. Programmed death ligand-1 expression in non-small cell lung cancer. Lab Invest. 2014;94:107–16. [PubMed: 24217091]
30. Wimberly H, Brown JR, Schalper K, Haack H, Silver MR, Nixon C, et al. PD-L1 Expression Correlates with Tumor-Infiltrating Lymphocytes and Response to Neoadjuvant Chemotherapy in Breast Cancer. Cancer Immunol Res. 2015;3:326–32. [PubMed: 25527356]
31. Gao J, Aksoy BA, Dogrusoz U, Dresdner G, Gross B, Sumer SO, et al. Integrative analysis of complex cancer genomics and clinical profiles using the cBioPortal. Sci Signal. 2013;6:
32. McLaughlin J, Han G, Schalper KA, Carvajal-Hausdorf D, Pelakanou V, Rehman J, et al. Quantitative Assessment of the Heterogeneity of PD-L1 Expression in Non–Small-Cell Lung Cancer. JAMA oncology 2016;2:46–54. [PubMed: 26562159]
33. Katz JB, Muller AJ, Prendergast GC. Indoleamine 2,3-dioxygenase in T-cell tolerance and tumoral immune escape. Immunol Rev. 2008;222:206–21. [PubMed: 18364004]

Statement of translational relevance:

Blockade of the PD-1 axis reinvigorates the anti-tumor immune response and induces clinical benefit in nearly 20% of patients with advanced lung cancer. The presence of PD-L1 (or B7-H1) in the tumor is associated with increased benefit to these therapies. The association and biological role of additional and potentially actionable immune inhibitory targets in lung cancer is not well understood. By quantitatively measuring PD-L1, B7-H4, IDO-1 and different immune cell subsets we show that lung carcinomas display limited co-expression of these immune suppressive markers. The presence of the markers in lung tumors is also differentially associated with immune infiltration and specific tumor features. Our data suggest that lung malignancies use preferentially discrete and non-overlapping routes to evade immunity that could participate in immunotherapy resistance. These results could support the design of clinical studies using biomarker-driven immunotherapies.

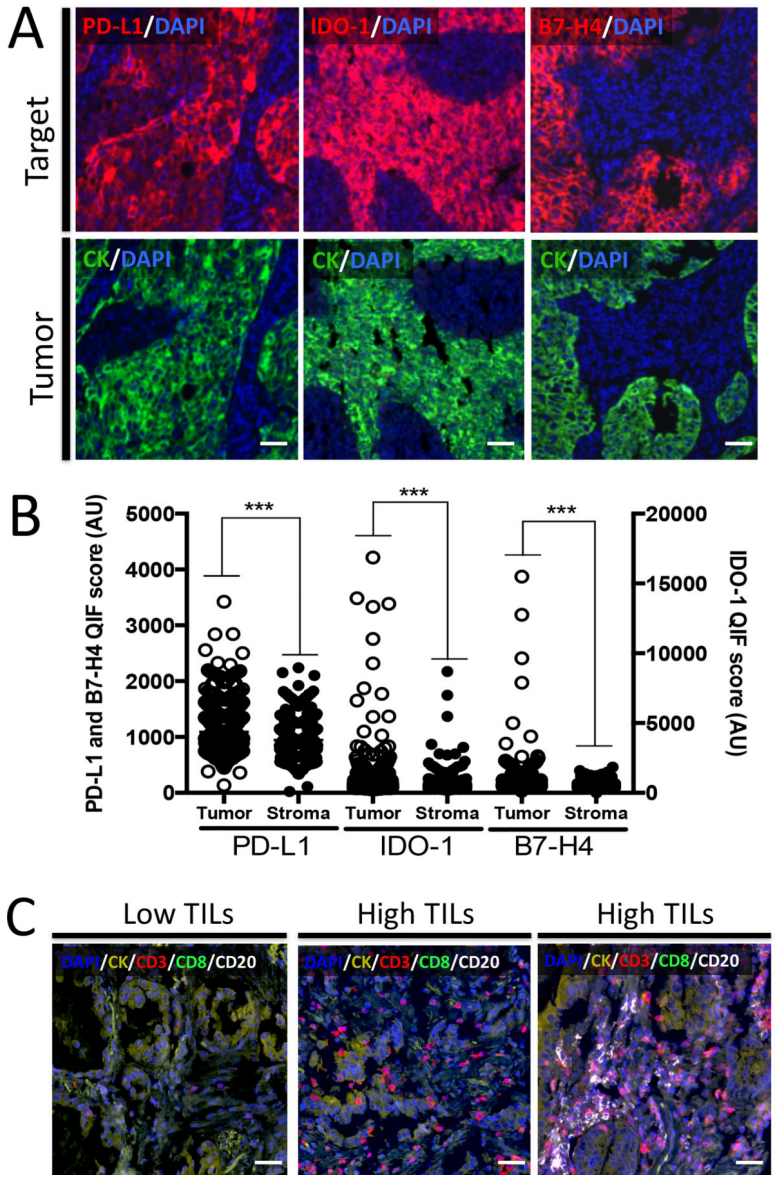

Figure 1. Detection of PD-L1, IDO-1, B7-H4 and TIL subsets using multiplex quantitative immunofluorescence (QIF) in lung cancer.

A) Representative fluorescence images showing the simultaneous detection of PD-L1, IDO-1 or B7-H4 (red fluorescence channel) and cytokeratin (green channel) in lung cancer samples using QIF. The upper panel shows tumors that are positive for each of the markers and the lower panel shows the cytokeratin positivity in the same samples. The target protein is indicated with red colored text in each figure. Green indicates the cytokeratin positive compartment and blue designated the DAPI positive nuclei. **B)** Levels of PD-L1, IDO-1 and B7-H4 in the tumor and stromal compartment of lung carcinomas from the studied cohorts. Each dot indicates the QIF level of the marker in a different tumor sample. ***=P<0.001. **C)** Representative fluorescence images showing the detection of TIL subsets in lung cancer samples by simultaneous staining of DAPI, cytokeratin (CK, yellow channel), CD3 (red channel), CD8 (green channel) and CD20 (white channel). Cases with low TILs (left panel),

high TILs with predominant CD3+ T-cells (center panel) and with high CD3 and CD20+ B lymphocytes (right panel) are presented. Bar=100 μm.

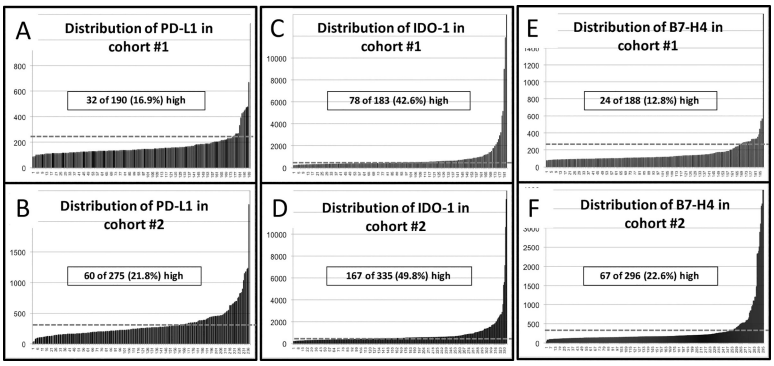

Figure 2. Levels of PD-L1, IDO-1 and B7-H4 in lung cancer.

A-F) Distribution of PD-L1, IDO-1 and B7-H4 QIF scores in lung cancer samples from cohort #1 **(A, C, E)** and cohort #2 **(B, D, F).** Scores are expressed as arbitrary units of fluorescence and the dashed gray line indicates the signal detection threshold determined as described in the methods section. The proportion of cases with detectable target signal is indicated within each chart.

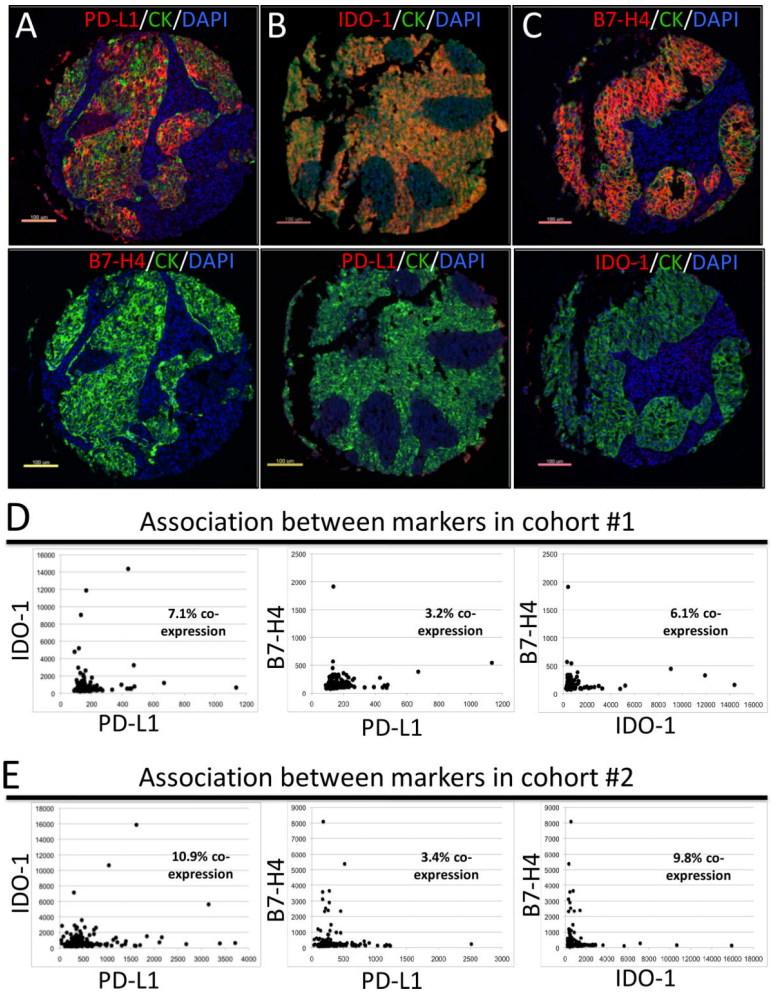

Figure 3. PD-L1, IDO-1 and B7-H4 are infrequently co-expressed in lung cancer.

A-C) Representative fluorescence pictures showing lung carcinomas with mutually exclusive expression of PD-L1, IDO-1 and B7-H4. The same tumors were stained for the different markers and the results are shown in the upper and lower panels. The target protein is indicated in the red fluorescence channel and tumor cells are highlighted with cytokeratin (CK, green fluorescence channel). Nuclei are stained with DAPI. **D-E)** Histograms showing the levels of PD-L1, IDO-1 and B7-H4 protein in lung carcinomas from cohort #1 **(D)** and cohort #2 **(E)**. The proportion of cases showing co-expression of the markers based on the signal detection threshold (see methods section) are indicated within each chart.

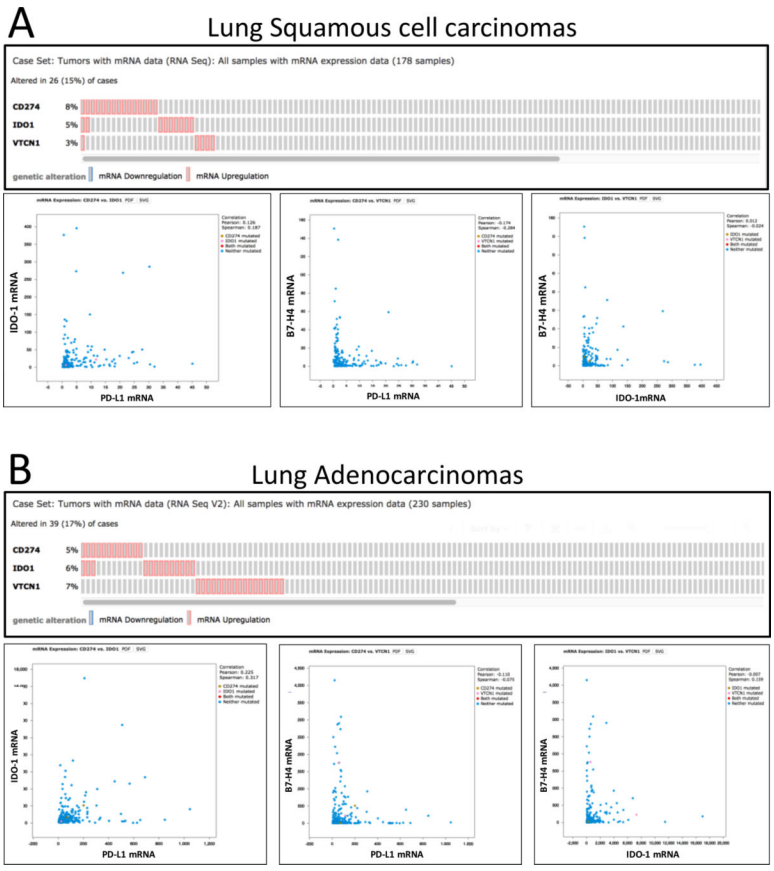

Figure 4.

PD-L1, IDO-1 and B7-H4 mRNA are infrequently co-expressed in lung cancer. Histograms showing the co-expression (upper charts) and levels (lower charts) of PD-L1, IDO-1 and B7-H4 mRNA transcripts in lung cancer cases from the TCGA lung squamous carcinoma **(A,** N=178**)** and lung adenocarcinoma **(B,** N=230**)** datasets. Levels of target mRNAs were measured using RNA-sequencing in whole tissue section samples and obtained through the cBioportal analysis platform.

Table 1.

Association between PD-L1, IDO-1, B7-H4, TILs and clinico-pathological variables in cohort #1

Parameter	Stratification	PD-L1 low	PD-L1 high	*P*	IDO-1 low	IDO-1 high	*P*	B7-H4 low	B7-H4 high	*P*
Sex	**Male**	73	18	0.329	50	38	0.981	75	15	0.136
	Female	83	14		53	40		87	9	
Age	**<70y**	106	22	0.891	76	57	0.168	115	13	0.116
	>70y	51	10		38	21		48	11	
Stage	**I-II**	108	25	0.302	69	58	0.281	118	13	0.071
	III-IV	48	7		34	20		44	11	
Histology	**ADC**	112	16	**0.006**	75	50	0.111	114	12	**0.041**
	SCC	26	7		17	14		24	9	
	Other	12	9		7	13		19	2	
CD3	**Low**	86	10	**0.011**	62	31	**0.009**	82	14	0.444
	High	72	22		43	47		82	10	
CD8	**Low**	85	10	**0.017**	60	32	**0.031**	79	16	0.085
	High	73	22		45	46		85	8	
CD20	**Low**	89	9	**0.004**	63	34	**0.013**	87	13	0.894
	High	72	23		45	50		85	12	

Table 2.

Association between PD-L1, IDO-1, B7-H4, TILs and clinico-pathological variables in cohort #2

Parameter	Stratification	PD-L1 low	PD-L1 high	*P*	IDO-1 low	IDO-1 high	*P*	B7-H4 low	B7-H4 high	*P*
Sex	**Male**	168	57	**0.005**	146	139	0.289	190	59	0.261
	Female	31	2		16	22		32	6	
Age	**<70y**	157	50	0.377	131	132	0.791	186	50	0.271
	>70y	40	9		30	28		35	14	
Stage	**I-II**	112	42	**0.031**	92	100	0.293	135	37	0.527
	III-IV	85	16		69	59		82	27	
Histology	**ADC**	83	19	0.068	62	64	0.323	102	12	**<0.0001**
	SCC	99	29		87	76		95	46	
	Other	16	11		13	20		25	6	
CD3	**Low**	115	18	**0.0003**	98	66	**0.0004**	109	39	0.125
	High	90	42		69	101		120	28	
CD8	**Low**	121	16	**<0.0001**	102	63	**<0.0001**	108	39	0.111
	High	84	44		65	104		121	28	
CD20	**Low**	114	23	**0.012**	109	62	**<0.0001**	115	37	0.6842
	High	91	37		61	111		118	34	